

Section 6

Developments in global forecast models, case studies, predictability investigations, global ensemble, monthly and seasonal forecasting

Adaptive deployment of balloons within HyMeX.

A. Doerenbecher^e and C. Basdevant^d
alex.doerenbecher@meteo.fr

1. Introduction

The BAMED^a project contributes to the international and multidisciplinary project HyMeX^b. BAMED, which is supported by the CNES^c, also involves the LMD^d and the CNRM^e. The project deals with atmospheric boundary layer drifting balloons to be deployed during the SOP (Special Observation Period) of HyMeX (in 2012 and 2013). The scientific objective for both LMD and CNRM is to prepare a deployment strategy, which is relevant for the needs of HyMeX. This strategy includes the selection of some launching sites and the development of a so-called targeting guidance tool that helps for the launching decisions in real-time. Indeed, the deployment of the balloons will be tailored for the numerical weather prediction (NWP) at various scales (sub-synoptic and mesoscale). The balloons are “Boundary Layer Pressurized Balloon” (BLPB) and “Aéroclippers”. Both types are designed and built by CNES. The paper will start by describing the HyMeX context and the balloons. Then some considerations about the launching sites will be considered prior to a sketch of the guidance system to be implemented in HyMeX.

2. Experimental context

2.1 HyMeX

The HyMeX project aims to better monitor the hydrological water cycle in the Mediterranean basin at various scales and in each compartment of the system: atmosphere, ocean and at the continental interface (hydrology). The scales to be studied stretch from very short (e.g. flash floods) to long range (e.g. ocean deep circulation). To enable such a monitoring, various observing strategies are combined with dedicated modelling efforts. “Long”, “enhanced” and “special observing periods” are embedded. The SOPs focus on intense events of limited duration (a few hours to a few days).

- SOP 1 (September/October 2012, North-Western basin) documents heavy precipitation events (HPE). Balloons will sample the moist low-level air flow converging toward the convective areas.
- SOP 2 (February-March 2013, North-Western basin): documents dense water formation related to strong regional winds (Mistral and Tramontana) that lead to the onset of deep oceanic convection. Balloons will sample fluxes at sea surface at the southern limit of the Gulf of Lion.

2.2 The aerostats (see also diagrams on figure 1).

The balloons prepared in BAMED will be deployed during SOPs. BLPBs drift at a constant density level, in the range of 925-850 hPa. These balloons have been designed to resist the heavy rain episodes likely to occur along their trajectories above the Mediterranean Sea. A shelter contains sensors for pressure, temperature, humidity and GPS positioning (additional instrumentation is possible). The wind will be deduced from sequential positions as the BLPBs have Lagrangian trajectories. The Aéroclipper consists of an airship-shaped balloon towing a marine gondola at the ocean surface. The guide rope between the two bodies is about 30 meters long and holds the sensors that indirectly collect ocean surface fluxes. The wind is measured, as these balloons have not a Lagrangian drift, due to the surface drag from the marine gondola.

3. Launching site selection

These balloons will be deployed above the Mediterranean Sea, which is the least observed atmospheric area within the North-Western basin. They will collect in-situ observations in the flow upstream of the

^aBAMED = **B**alloons in the **M**editerranean

^bHyMeX = **H**ydrological cycle in the **M**editerranean **E**xperiment (<http://www.hymex.org/>)

^cCNES = **C**entre **N**ational des **É**tudes **S**patiales (<http://www.cnes.fr/>)

^dLMD = **L**aboratoire de **M**étéorologie **D**ynamique (<http://www.lmd.jussieu.fr/>)

^eCNRM = **C**entre **N**ational de **R**cherche **M**étéorologiques, Météo-France, Toulouse (<http://www.cnrm.meteo.fr/>)

events of interest. Thus the collected data are expected to be of great interest for the NWP, especially the high-resolution mesoscale models to be implemented during HyMeX (e.g. AROME West-Med). As a consequence, the balloons will transmit the data in near real-time. Moreover, the balloons launch strategy should optimize both the impact of the data in the NWP and the logistical constraints. It is crucial to choose the launching sites that are the most propitious to reach HyMeX targets. A selection of alternative sites spread around the western Mediterranean basin has been evaluated with trajectories simulated on a series of past cases. The meteorological data used were both analyses and forecast compute either with ECMWF or Météo-France global model or with high-resolution model. The trial implied to define targets within the weather events and to maximize the number of trajectories reaching these targets together with their length and to minimize the loss of platforms. The statistics showed that a launching site in the Balearic Islands such as Mahòn in Minorca is a good trade-off for the SOP 1. A site on the French coasts close to Montpellier would be the ideal solution for the SOP 2.

4. Targeting guidance

As for any field campaign in which specific phenomena ought to be chased with limited observing resources, an adaptive observation strategy is worth being used to increase the rate of success. This strategy may include a decision-making tool. A trajectory simulator and a targeting tool developed respectively LMD and CNRM will be interfaced to produce a guidance to be sent to the field teams, in order to help them preparing the balloons and launching them at most propitious time. The diagram 2 sketches the system to be built and implemented at the HyMeX operation centre.

Conclusions

The BAMED project allowed capitalizing on the CNES know-how with the low-level drifting balloons that were deployed within prior field campaigns such as VASCO^f, CIRENE^f or AMMA⁹. The novelty is to chase specific phenomena within a real-time data collection system supporting numerical environmental prediction.

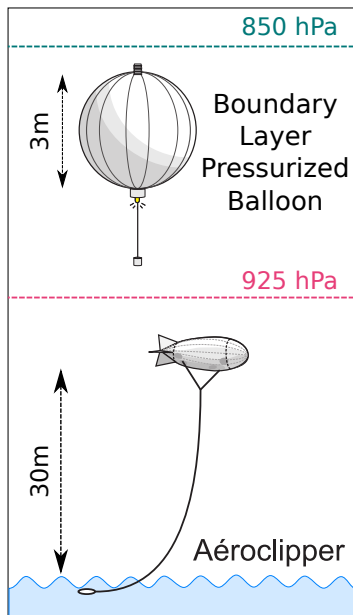


Figure 1: Drifting balloons to be deployed by the CNES during HyMeX.

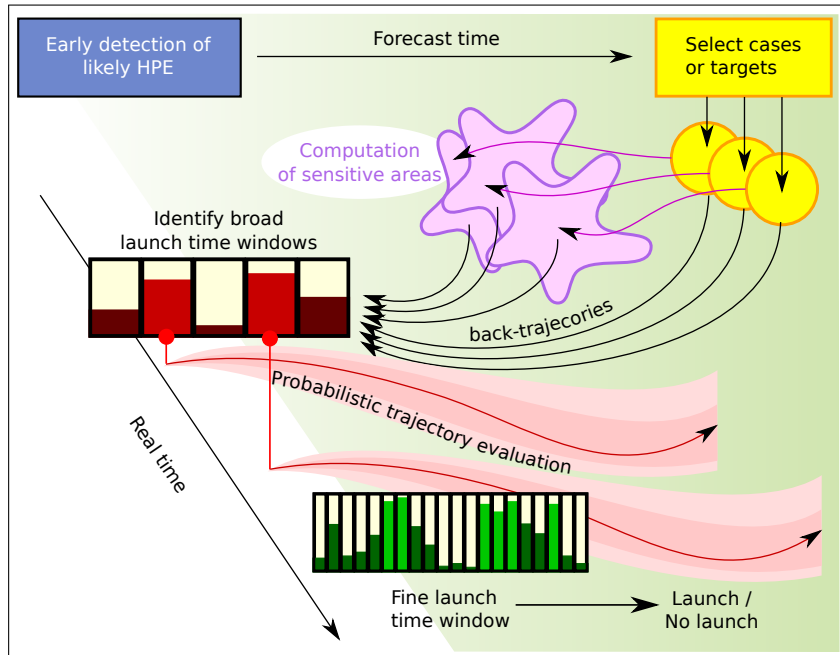


Figure 2: Principle of the launching guidance tool to be implemented in the SOPs of HyMeX

^f<http://www.lmd.ens.fr/vasco/>

⁹ African Monsoon Multiscale Analysis (<http://www.amma-international.org/>)

The reduced grid with variable latitude resolution for the global semi-Lagrangian numerical weather prediction model

Fadeev R. Yu.

*Institute of Numerical Mathematics, Russian Academy of Sciences,
and Hydrometcentre of Russia, Moscow RUSSIA
email: fadeev@inm.ras.ru*

It is well known that the parameterizations of sub-grid processes in the forecast model may work incorrectly on the non-isotropic grid. To avoid such an obstacle we developed an approach to construct the longitude-latitude reduced grid with variable latitude resolution suitable for semi-Lagrangian finite difference models.

The quasi-uniform grid on the Earth surface imposes some constraints on the steps within the region under consideration. Therefore the iterative method of grid generation implies following restrictions on the grid step ratio: $\max(\Delta\phi/(\Delta\lambda \cos(\phi)), \Delta\lambda \cos(\phi)/\Delta\phi) \leq C(\phi) + \delta C$ and $\Delta_j\phi/\Delta_{j+1}\phi \leq R$. Beginning with the uniform (in both latitude and longitude) grid we construct a one-dimensional latitude mesh which is used for the reduced grid generation. Then we diminish δC and continue this procedure.

Our technique of latitude mesh generation is based on the physical analogy between a simplex mesh and the truss structure [2] where meshpoints are nodes of the truss. Assuming an appropriate force-displacement function for the bars in the truss we determine the equilibrium of this system. The latitudinal grid steps with high resolution in the vicinity of Novosibirsk (in latitude 55° North) are shown in Fig. 1a.

The main goal of the reduced grid construction method is to minimize the total number of the grid nodes at the fixed upper limit ϵ_Ψ for the sum of the r. m. s. interpolation error of a given function f_k^0 ($k = 1, \dots, n_k$):

$$\Psi = \sum_{j=1}^{n_\phi} \sum_{k=1}^{n_k} \int_0^{\pi/2} |f_k(\lambda, \phi_j) - f_k^0(\lambda, \phi_j)|^2 \cos(\phi_j) d\lambda, \quad \Psi \leq \epsilon_\Psi \quad (1)$$

Here $f_k^0 = \cos\left(\phi^* \frac{n_\phi}{10}\right) \cos\left(\lambda^* \frac{n_\lambda}{10} + \frac{\pi}{2} \frac{k}{n_k}\right)$, where (ϕ^*, λ^*) are coordinates in the rotated system with North pole at $(55^\circ, 45^\circ)$ with respect to regular coordinate system (ϕ, λ) .

Equation (1) is solved numerically for each value of ϵ_Ψ and the grid obtained in such a way we call as the optimal reduced grid. It should be noted that the properties of such a grid substantially depend on the function f_k^0 . Normalized values of the grid steps $\Delta\phi$ and $\Delta\lambda$ as a function of latitude ϕ are shown in Fig. 1b. Small disturbances on the lower curve (the longitudinal step) are due to the restriction on the number of longitudinal grid points $n_\lambda(\phi)$ because it is the product of $2^n \cdot 3^m \cdot 5^l$ (where $n \geq 2, m \geq 0, l \geq 0$).

We carried out a number of shallow–water tests [4] that involve both the solid–body rotation of a cosine bell around the sphere through the poles and two cases of the deformational flow tests. In all cases our method of grid generation was found to be promising. It should be noted that the error of the numerical solution obtained on the reduced grid with uniform latitude resolution is somewhat higher in comparison with that presented in [1].

This method will be used for construction of the grid for the new version of the weather prediction SL–AV global model [3] with conservative semi–Lagrangian scheme. Latitudinal derivatives in this model are calculated in the space of longitudinal Fourier coefficients, so that the reduced grid can be implemented.

Advantage of our method is that it allows us to take into account various details of the weather prediction model and to apply additional restrictions on the grid. This work was supported by the RFBR grant 10-05-01066.

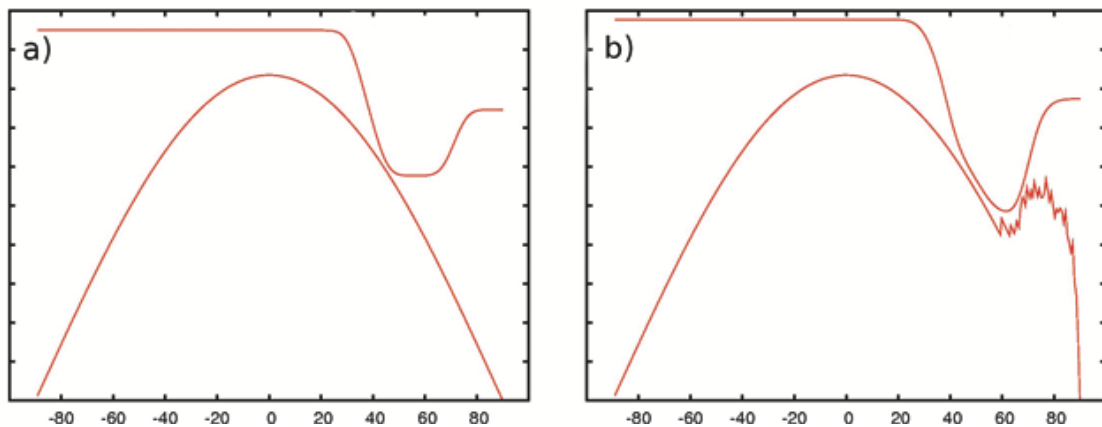


Figure 1: Normalized latitudinal (upper curve) and longitudinal (lower curve) steps after first iteration (a) and when the iteration convergence criterion is achieved (b).

References

- [1] Fadeev R. Yu. Reduced latitude–longitude grid constructing for the global numerical weather prediction. – Russ. Meteor. and Hydrol., 2006, N 4, pp. 5–20.
- [2] Persson P.–O., Strang G., A Simple Mesh Generator in MATLAB. SIAM Review, Volume 46 (2), pp. 329–345, June 2004
- [3] Tolstykh M. A. Semi–Lagrangian high resolution model of atmosphere for numerical weather prediction. – Russ. Meteor. and Hydrol., 2001, N 4, pp. 1–9.
- [4] Williamson D. L., Drake J.B., et al. A standart test set for numerical approximations to the shallow water equations in spherical geometry. – J. Comput. Phys., 1992, vol. 102, pp. 211–224.

Modification to Initial Perturbations of JMA's Typhoon Ensemble Prediction System

Yoichiro Ohta

Numerical Prediction Division, Japan Meteorological Agency

e-mail:ota@met.kishou.go.jp

Since February 2008, JMA has operated the Typhoon Ensemble Prediction System (TEPS) to contribute to operational five-day forecasts of tropical cyclones (TCs) at the RSMC Tokyo-Typhoon Center. The TEPS forecast model is a low-resolution version (TL319L60) of JMA's Global Spectral Model (GSM), and is operated four times a day when TCs are present or expected to appear in JMA's area of responsibility ($0^{\circ}\text{N} - 60^{\circ}\text{N}$, $100^{\circ}\text{E} - 180^{\circ}\text{E}$). There are 11 TEPS members (1 control member + 10 perturbed members), and the forecast time is up to 132 hours. A detailed description of the TEPS is given by Yamaguchi and Komori (2009).

The initial perturbations of the TEPS are produced using the singular vector (SV) method (Buizza and Palmer 1995). Two spatial target areas to obtain SVs are defined to capture the uncertainty of TC track forecasts. One is the Northwestern Pacific ($20^{\circ}\text{N} - 60^{\circ}\text{N}$, $100^{\circ}\text{E} - 180^{\circ}\text{E}$), and the other consists of a group of areas around the central positions of TC forecasts (three at maximum: TC target area). To improve the forecast skill of the TEPS, JMA introduced two revised methods for the production of initial perturbations in May 2010. First, the TC target areas are set as circular regions with a 750-km radius from the TC's central position, in contrast to the previous rectangular-area settings (10 degrees in the meridional direction and 20 degrees in the zonal direction). Figure 1 shows a comparison of the previous and new TC target areas centered on the position of 20°N and 140°E . Second, the amplitude of initial perturbations is normalized using a moist total energy (Ehrendorfer et al. 1999; Barkmeijer et al. 2001) value, in contrast to the previous normalization that used the maximum meridional or zonal wind speed.

Figure 2 shows ensemble mean track forecast errors classified according to reliability indices. A, B and C represent higher, middle and lower levels of forecast reliability, respectively. The indices are determined by six-hourly accumulated ensemble spreads at each forecast time. In the new system, the mean track forecast errors of A, B and C are maintained in the same order throughout the forecast time, unlike in the previous system. This indicates that the modifications implemented contribute to the appropriate distribution of initial perturbations. Consequently, the spread-skill relationship of TC track forecasts is improved, and the TEPS is able to provide more accurate information on operational TC forecasts.

References

- Barkmeijer, J., R. Buizza, T. N. Palmer, K. Puri, and, J.-F. Mahfouf, 2001: Tropical singular vectors computed with linearized diabatic physics. *Quart. J. Roy. Meteor. Soc.*, **127**, 685 – 708.
- Buizza, R. and T. N. Palmer, 1995: The singular-vector structure of the atmospheric global circulation. *J. Atmos. Sci.*, **52**, 1434 – 1456.

Ehrendorfer, M., R. Errico, and K. Raeder, 1999: Singular vector perturbation growth in a primitive equation model with moist physics. *J. Atmos. Sci.*, **56**, 1627 – 1648.

Yamaguchi, M. and T. Komori, 2009: Outline of the Typhoon Ensemble Prediction System at the Japan Meteorological Agency. *RSMC Tokyo-Typhoon Center Technical Review*, **11**, 14 – 24.

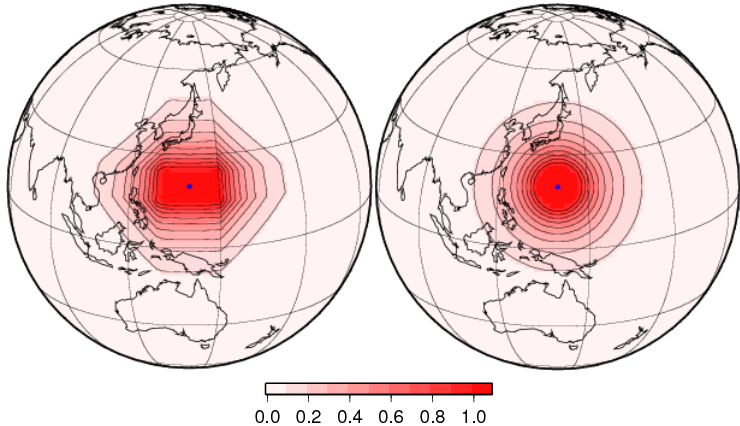


Figure 1 Comparison of the previous (left) and new (right) TC target areas. The central position of the targets is 20°N and 140°E. Colors with contours show projection operator values in the SV calculation.

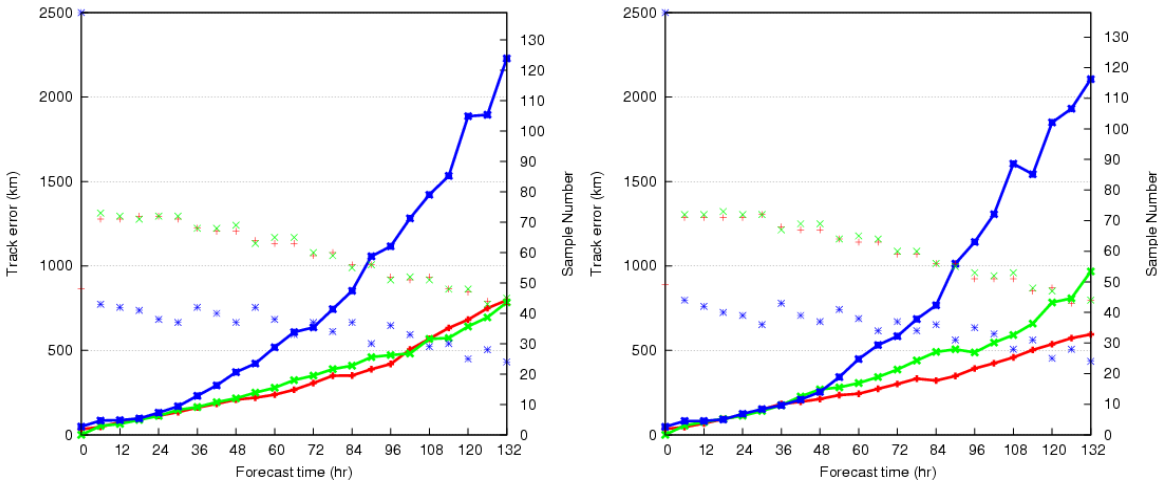


Figure 2 Ensemble mean track forecast errors for TCs in JMA's area of responsibility from 25 September to 25 October, 2009. The left and right panels are for the old and new systems, respectively. The red, green and blue lines show the mean track errors with reliability indices of A, B and C, respectively. The colored marks indicate the number of samples for each class.

A Stochastic physics scheme for model uncertainties in the JMA one-week Ensemble Prediction System

Hitoshi Yonehara and Masashi Ujiie
 Numerical Prediction Division, Japan Meteorological Agency
 e-mail: yonehara@met.kishou.go.jp

1 Introduction

Since 2001, the Japan Meteorological Agency (JMA) has operated the one-week Ensemble Prediction System (WEPS). On 16 December, 2010, it began employing a stochastic physics scheme as a model ensemble method and reduced the amplitude of the initial perturbations over the Tropics. This paper outlines and reports on the performance of the new WEPS.

2 Implementation of a stochastic physics scheme into JMA's WEPS

In the current WEPS, the Singular Vectors (SVs) method (Buizza and Palmer, 1995) is used as the initial perturbations generator. Table 1 outlines the specifications of the SVs method in the WEPS.

Table 1: Specifications of the initial perturbations generator.

	Northern Hemisphere	Tropics
Targeted region	30°N-90°N	20°S-30°N
Resolution of tangent-linear and adjoint model	T63L40	
Physical processes	Initialization, horizontal diffusion, surface and vertical turbulent diffusion	Full physics processes
Optimization time	48 hours	24 hours
Norm	Moist total energy	
Amplitude of initial perturbation	12% of the climatological temperature variance at the 500hPa level	24% of the climatological temperature variance at the 850hPa level

The stochastic physics scheme (Buizza et al., 1999) was newly introduced into the operational WEPS. This scheme represents random errors associated with parametrized physical processes as follows:

$$\frac{\partial \mathbf{x}}{\partial t} = F(\mathbf{x}) + \alpha(\lambda, \phi, t)P(\mathbf{x})$$

where t , \mathbf{x} , $F(\mathbf{x})$ and $P(\mathbf{x})$ are the time, the set of forecast variables, the total tendency of the forecast model and the tendency of the parametrized physical processes, respectively. λ and ϕ show latitude and longitude; $\alpha(\lambda, \phi, t)$ is a random variable described in a spectral space (Berner et al. 2009), featuring spatial correlation with a total wave number of 20 and a time correlation of six hours. The average of α is set to zero. Its value is limited to the range from -0.7 to 0.7 to avoid excess perturbations, and its value in the stratosphere also is set to zero. The whole globe is perturbed by the scheme in initially perturbed forecasts. The unperturbed forecast is conducted without the stochastic physics scheme.

Concurrently with the introduction of model error perturbations, we also reduced the amplitude of the initial perturbations from 28% to 24 % of the climatological temperature variance at the 850hPa level over the Tropics (20°S-30°N). This modification was employed to reduce the occurrence of unrealistic initial states of specific humidity over the region.

3 Performance of the new WEPS

To assess the performance of the new WEPS, preliminary experiments were carried out for boreal summer and winter. Hereafter, the experiments with and without the stochastic physics scheme are referred to as WITH and W/O respectively. Figure 1 shows the spread and root mean square error (RMSE) of the experiments over the Tropics (20°S-20°N) in August 2007. The spread of temperature at the 850 hPa level (T850) in WITH increases greatly over the Tropics (Figure 1(a)) in comparison to that of W/O. Figures 1(b) and 1(c) also show that the ratio $\left(\frac{m+1}{m-1} \frac{\text{spread}^2}{\text{RMSE}^2}\right)$, where m is the number of members) of WITH is also closer to one than that of W/O. These impacts result from the introduction of model error perturbations and the alleviation of the inadequacy of spread to RMSE. Figure 2 shows the receiver operating characteristic (ROC) area and the Brier skill score (BSS) for the probability of cases in which the T850 anomaly over the Tropics is larger (i.e., high temperature events) and smaller (i.e., low temperature events) than 1.5 and -1.5 times of climatological standard deviation. The verification period is the same as that for Figure 1. For high-temperature events, both the ROC and BSS of WITH are superior to W/O for all forecast times. For low-temperature events, the improvement of WITH is more obvious after forecast time of 24 hours. In winter, WITH also shows better BSS values than W/O (not shown).

The results indicate that the new WEPS has positive impacts on both deterministic and probabilistic forecasts especially in the summer season.

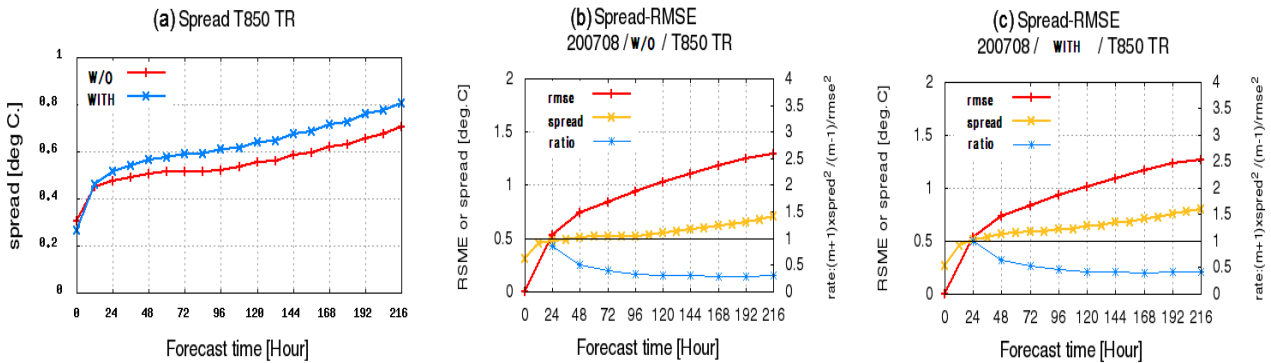


Figure 1: (a) comparison of spread and RMSE for the Tropics (20°S-30°N) between the two experiments in August 2007, (b) relationship of spread (yellow line) and RMSE (red line) and their ratio (blue line) of T850 over the Tropics for WITH, (c) same as (b) but for W/O. The ratio is defined as $\frac{m+1}{m-1} \frac{\text{spread}^2}{\text{RMSE}^2}$ where m is the number of ensemble members.

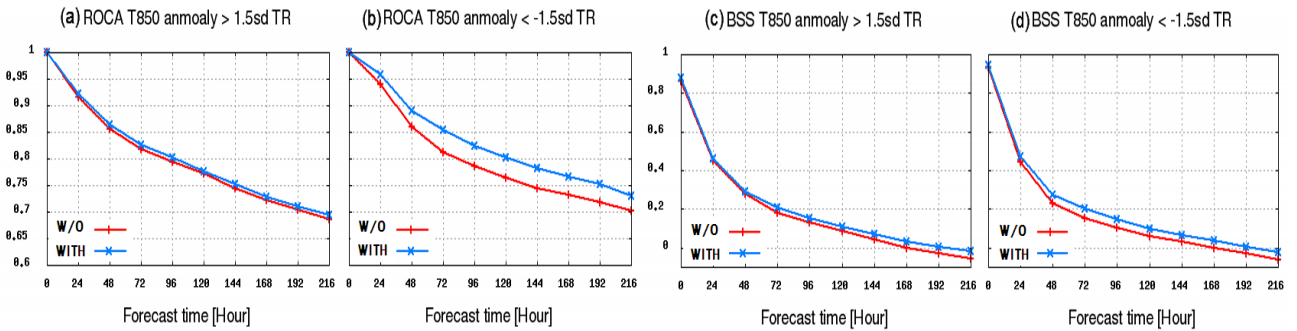


Figure 2: ROC area for the probability of T850 anomalies (a) above 1.5 and (b) below -1.5 times of climatological standard deviation over the Tropics (20°S-20°N) in August 2007. (c), (d) same as (a), (b) but for Brier skill score.

References

Berner, J. and co-authors, 2009: A Spectral Stochastic Kinetic Energy Backscatter Scheme and Its Impact on Flow-Dependent Predictability in the ECMWF Ensemble Prediction System. *J. Atmos. Sci.*, **66**, 603-626

Buizza, R. and Palmer T.N., 1995: The singular vector structure of the atmosphere global circulation. *J. Atmos. Sci.*, **52**, 1434-1456

Buizza, R., and co-authors, 1999: Stochastic representation of model uncertainties in the ECMWF Ensemble Prediction System. *Quart. J. Roy. Meteor. Soc.*, **125**, 2887-2908